IDENTIFICATION OF NON LINEAR MODELS OF UNMANNED UNDERWATER VEHICLES: COMPARISON BETWEEN TWO IDENTIFICATION METHODS

A. El-Fakdi*, A. Tiano†, P. Ridao*, J. Batlle*

* *Institute of Informatics and Applications*
University of Girona, Spain

† *Department of Information and Systems*
University of Pavia, Italy

Abstract: This paper presents a comparison between two identification methods for the off-line identification of non linear models of Unmanned Underwater Vehicles (UUV's), one based on the minimization of the acceleration prediction error (classic method) and another based on the minimization of the velocity one step prediction error (new method). Both methods are compared through its application to the identification of the dynamic model of URIS UUV. Results suggest that better models can be obtained using the proposed method

Keywords: Identification, parameter estimation, numerical methods, unmanned underwater vehicles.

1. INTRODUCTION

The application of system identification techniques to naval vehicles is concerned with the estimation, on the basis of experimental measurements, of a number of parameters or of hydrodynamic derivatives that characterise the vehicle's dynamics (Abkowitz, 1980). Such measurements, collected during full-scale trials by the on-board sensors, are processed by a parameter estimation routine (Ljung, 1987).

The identification methods that, in the recent years, have been proposed for UUV identification generally operate off-line and the underlying mathematical models are of the scalar type. Furthermore, they are essentially deterministic, since the effects of disturbances affecting the UUV dynamics and of measurement noise are not taken into consideration (Caccia, et al., 2000). An on-line deterministic identification method that has been most recently proposed (Smallwood and Whitcomb, 2001) is limited to scalar decoupled models.

Most of methods used for identification of the uncoupled dynamics equation of an UUV are based on the minimization of the acceleration prediction error, usually applying LS estimation techniques (in the following we will call this method "the classical" method) (Ridao, 2001). Recently we proposed to carry out the identification using the one step integral of the dynamics equation (Tiano, 2002 & Carreras, 2003). In this case LS is used to estimate the model parameters which minimize the one step prediction error of the velocity (in the following we will call this method "the new" method). In this paper we compare the results obtained with both methods, through exhaustive experimentation with URIS UUV. (See Fig. 1).

A brief review of the UUV mathematical models generally used in the literature is presented in sub-section 1.1 of this paper. In section 2 the two methods of identification used are presented, the classic and the new one. In section 3 a description of URIS underwater robotic vehicle is reported and, in section 4, the comparison of the identification results obtained with both methods for the identification of URIS surge DOF are shown, also we expose the results for the other identified DOF's: pitch and yaw. Finally some concluding remarks are done in section 5.

1.1 UUV Mathematical models

As described in the literature (Fossen, 1994), the non-linear hydrodynamic equation of motion of an underwater vehicle with 6 DOF, in the body fixed frame, can be conveniently expressed as:

$$\begin{aligned} {}^{B}\tau + G(\eta) - D\left({}^{B}\upsilon\right){}^{B}\upsilon + \tau_p = \\ \left({}^{B}M_{RB} + M_A\right)\cdot {}^{B}\dot{\upsilon} + \left({}^{B}C_{RB}({}^{B}\upsilon) + C_A\left({}^{B}\upsilon\right)\right)\cdot {}^{B}\upsilon \end{aligned} \quad (1)$$

Identification of the complete set of coefficients and hydrodynamic derivatives which appear in Equation (1) is a rather complex task. The identification problem can be much more easily approached if the following simplifications are applied:

- $D({}^{B}v)$ consists of the lineal and quadratic damping forces and can be assumed diagonal.
- ${}^{B}M_{RB}$ and ${}^{B}M_{A}$ can be assumed diagonal (this is true for URIS UUV due to its spherical shape see section 3).
- the body frame is located at the gravity centre

Moreover, if the robot is actuated in a single DOF during the identification experiments, further simplifications can be carried out. For instance, let's consider the dynamic equation for the surge DOF:

$$X+(\sin\theta B-\sin\theta W)-(X_u+X_{u|u|}|u|)\cdot u+\tau_p= \\ (m-X_{\dot u})\cdot\dot u+[(m-Z_{\dot w})\cdot wq]-[(m-Y_{\dot v})\cdot vr] \quad (2)$$

which follows the standard notation proposed in (Fossen, 1994). If we excite the robot in a single DOF, surge in this case, in such a way that:

- $u\neq 0$ *and* $v=w=p=q=r=0$
- $\theta=\phi=0$

then we run an uncoupled experiment so, equation (2) can be rewritten as:

$$\dot u=\underbrace{\frac{X}{(m-X_{\dot u})}}_{\gamma}-\underbrace{\frac{X_u}{(m-X_{\dot u})}}_{\alpha}\cdot u-\underbrace{\frac{X_{u|u|}|u|}{(m-X_{\dot u})}}_{\beta}\cdot u+\underbrace{\frac{\tau_p}{(m-X_{\dot u})}}_{\delta} \quad (3)$$

The same procedure can be applied to each degree of freedom so we can consider a generic uncoupled equation of motion for the *i*-degree as:

$$\dot x_i=\alpha_i x_i+\beta_i x_i|x_i|+\gamma_i\tau_i+\delta_i \quad (4)$$

where the state variable *x* represents speed. Hence, things become easier if we use equation (4) for the identification.

2. IDENTIFICATION METHOD

2.1 Classic method

Equation (4) can be expressed as an equation linear in the vector of unknown parameters:

$$\underbrace{\begin{bmatrix}\dot x_{i,1}\\ \dot x_{i,2}\\ \cdots\\ \dot x_{i,n}\end{bmatrix}}_{y(t)}=\underbrace{\begin{bmatrix}x_{i,1} & x_{i,1}|x_{i,1}| & \tau_{i,1} & \eta_1\\ x_{i,2} & x_{i,2}|x_{i,2}| & \tau_{i,2} & \eta_2\\ \cdots & \cdots & \cdots & \cdots\\ x_{i,n} & x_{i,n}|x_{i,n}| & \tau_{i,n} & \eta_n\end{bmatrix}}_{H(x(t),\,\tau_i(t))}\cdot\underbrace{\begin{bmatrix}\alpha\\ \beta\\ \gamma\\ \delta\end{bmatrix}}_{\theta}+\underbrace{\begin{bmatrix}\varepsilon_{i,1}\\ \varepsilon_{i,2}\\ \cdots\\ \varepsilon_{i,n}\end{bmatrix}}_{\varepsilon} \quad (5)$$

where η it's a binary variable (value 0 or 1) which allows to take into account a bias term. Using the above equation, the LS estimation technique can be applied to estimate the vector of unknowns θ, through the application of the following equations:

$$\hat\theta_{LS}=(H^TH)^{-1}H^Ty \quad (6)$$

$$\hat\sigma_\theta=\sqrt{diag(\mathrm{cov}(\hat\theta_{LS}))} \quad (7)$$

$$\mathrm{cov}(\hat\theta_{LS})=\hat\sigma^2(H^TH)^{-1} \quad (8)$$

$$\hat\sigma^2=\frac{(y-H\hat\theta_{LS})^T(y-H\hat\theta_{LS})}{\dim(y)-\dim(\theta)} \quad (9)$$

2.2 New method

As it can be easily recognised, the UUV uncoupled dynamics, as expressed by Equation (4) is a particular case of a more general class of non linear system that are linear with respect to the system parameter vector. The system dynamics can be expressed by:

$$\dot x=\phi(x(t),\tau(t))\theta \\ y(t_k)=x(t_k)+e(t_k) \quad (10)$$

where $\phi\in R^{nxl}$ is a matrix valued function depending only on state and control vectors, while $\theta\in R^l$ is a constant and unknown parameter vector that characterises the system dynamics.
The identification problem consists of estimating the unknown parameter vector θ. According to the Output Prediction Error method (Ljung, 1987), identification of parameter vector θ is equivalent to the minimization of a scalar cost function of the form:

$$J(\theta)=\frac{1}{N}\sum_{k=1}^{N}\varepsilon^T(t_k)W^{-1}(t_k)\varepsilon(t_k) \quad (11)$$

The cost function is constituted by a weighted sum of squares of prediction errors $\varepsilon(t_k)$, which are the difference between the observed output vectors and the one-step prediction of the output $\hat y(t_k)$, i.e.:

$$\varepsilon(t_k)=y(t_k)-\hat y(t_k) \quad (12)$$

The positive definite matrices $\{W^{-1}(t_k)\}_{k=1}^N$ consist of weights that should take into account the reliability of measurements at each discrete time instant. It is worth noting that if the measurement noise vector $\varepsilon(t_k)$ is zero-mean then:

$$\hat y(t_k)=\hat x(t_k) \quad (13)$$

where $\hat x(t_k)$ denotes the expected state vector at time t_k. In order to determine a solution to the minimization of the cost function expressed by Equation (11), it is necessary that an estimate of one-step predicted output $\hat y(t_k)$ is available. For this purpose, let us formally integrate both sides of state equation in Equation (10) between two subsequent time instants t_{k-1} and t_k, obtaining:

$$x(t_k)-x(t_{k-1})=\Big[\int_{t_{k-1}}^{t_k}\phi(x(s),\tau(s))ds\Big]\cdot\theta \quad (14)$$

If, taking into account Equation (13), it is assumed that $x(t_{k-1})=\tilde y(t_{k-1})$, where $\tilde y(t_{k-1})$ is a properly filtered version of the output vector $y(t_{k-1})$, i.e. if we assign to the unknown state vector a corresponding filtered output, then we obtain the following estimate for the state vector at time t_k :

$$\hat x(t_k)=\tilde y(t_{k-1})+F_k\cdot\theta \quad (15)$$

where

$$F_k = \int_{t_{k-1}}^{t_k} \phi(\hat{x}(s), \tau(s))ds \tag{16}$$

and thus, we can compute the one-step prediction error of Equation (12) in the form:

$$\varepsilon(t_k) = \tilde{y}(t_k) - \tilde{y}(t_{k-1}) - F_k \cdot \theta \tag{17}$$

reordering Equation (17) we get:

$$\tilde{y}(t_k) - \tilde{y}(t_{k-1}) = F_k \cdot \theta + \varepsilon(t_k) \tag{18}$$

$$\begin{bmatrix} \tilde{x}_{i,1} - \tilde{x}_{i,0} \\ \tilde{x}_{i,2} - \tilde{x}_{i,1} \\ \dots \\ \tilde{x}_{i,k} - \tilde{x}_{i,k-1} \end{bmatrix} = \begin{bmatrix} \int_0^1 \tilde{x}_i dt & \int_0^1 \tilde{x}_i|\tilde{x}_i| dt & \int_0^1 \tau_i dt & \int_0^1 1 dt \\ \int_1^2 \tilde{x}_i dt & \int_1^2 \tilde{x}_i|\tilde{x}_i| dt & \int_1^2 \tau_i dt & \int_1^2 1 dt \\ \dots & \dots & \dots & \dots \\ \int_{k-1}^k \tilde{x}_i dt & \int_{k-1}^k \tilde{x}_i|\tilde{x}_i| dt & \int_{k-1}^k \tau_i dt & \int_{k-1}^k 1 dt \end{bmatrix} \bullet \begin{bmatrix} \alpha_i \\ \beta_i \\ \gamma_i \\ \delta_i \end{bmatrix} + \begin{bmatrix} \varepsilon_{i,1} \\ \varepsilon_{i,2} \\ \dots \\ \varepsilon_{i,k} \end{bmatrix} \tag{19}$$

$\tilde{y}(t_k) - \tilde{y}(t_{k-1})$ $\quad$ F_k $\quad$ θ $\quad$ ε

which is linear in the vector of unknown parameters admitting a unique solution that can be obtained through Least Squares (LS) algorithm:

$$\theta_{LS}(N) = (F^T(N) \cdot W^{-1}(N) \cdot F(N))^{-1} \cdot F^T(N) \cdot W^{-1}(N) \cdot Y(N) \tag{20}$$

3. DESCRIPTION OF URIS UUV

URIS robot was developed at the University of Girona with the aim of building a small-sized UUV. The hull is composed of a stainless steel sphere with a diameter of 350mm, designed to withstand pressures of 3 atmospheres (30 meters depth). Due to the stability of the vehicle in pitch and roll, the robot has four degrees of freedom (DOF): surge, sway, heave and yaw. Except for the sway DOF, the others DOFs can be directly controlled.

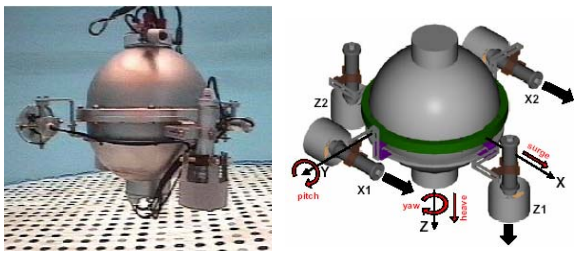

Fig. 1. (left) URIS in the tank. (right) URIS reference frame

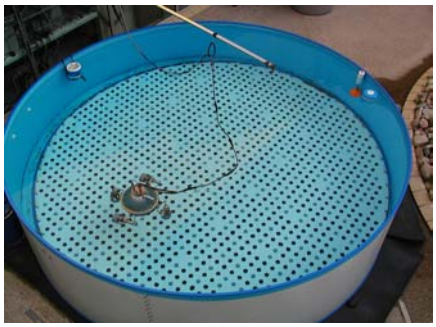

Fig. 2. Water tank used in the identification experiments.

4. RESULTS

In order to compare both methods, an extensive set of experiments was carried out. The trials took place in a small water tank (4m. diameter and 1m. depth) (see Fig. 2). A very accurate navigation system based on computer vision (Carreras, 2003) was used for the measurements. Due to the reduced dimension in depth, only the surge, yaw and pitch DOF's were identified.

4.1 Identification results for the surge DOF

Five different trials were run for the surge DOF, 4 using step signals and 1 using PBRS signals. Three of them (steps) where validated and 2 were discarded. In all cases, no significant improvement was observed taking into account the quadratic damping. For this reason, it was considered to be zero. This is usual for very low speed robots like the one considered here. Table 1 shows the results of the validated experiments using the new method as well as their average. Table 2 shows the results obtained applying the classic identification method. The estimated parameters are shown together with their standard deviation and the cost of the whole experiment.

Table 1 Parameter results for surge DOF (New)

Exp		α_x	γ_x	δ_x	J_x
1	θ	0.3243	0.0178	-0.0018	1.6305e-4
	σ	0.0023	0.0001	0.0002	
2	θ	0.3185	0.0201	0.0041	1.8948e-4
	σ	0.0016	0.0001	0.0001	
3	θ	0.3237	0.0173	0.0013	1.8918e-4
	σ	0.0016	0.0001	0.0002	
Mean	θ	0.3222	0.0184	0.0012	1.8057e-4
	σ	0.0018	0.0001	0.00016	

Table 2 Parameter results for surge DOF (Classical)

Exp		α_x	γ_x	δ_x	J_x
1	θ	0.4147	0.0236	-0.0010	1.8432e-4
	σ	0.0025	0.0001	0.0002	
2	θ	0.4790	0.0321	-0.0090	2.5973e-4
	σ	0.0022	0.0001	0.0002	
3	θ	0.5153	0.0295	0.0014	2.4150e-4
	σ	0.0021	0.0001	0.0002	
Mean	θ	0.4697	0.0284	-0.0028	2.28517e-4
	σ	0.00227	0.0001	0.0002	

Note that physical parameters of the vehicle can be easily computed from those shown in table 1 and 2 by applying equation (3). Lets us consider in the following paragraphs, experiment 2 as a case of study to illustrate the procedure. Fig. 3 shows the input signals (force and the filtered force, acceleration, speed and position) of the experiment. Figure 4 shows the one step prediction error of the velocity for both methods. It's clear that better results can be achieved with the new method. The statistical validation of the results for the new and classic method is reported in the figure 5. Note that the

standard deviation of the histogram of the new method is smaller than the one of the classic method and that better autocorrelation results are observed. The performance of the two methods is presented in Fig. 6 where the measured velocity is compared with the one step predicted velocity evaluated in the working point of the previous measured velocity (for both methods). Finally figure 7 show the long term simulation capability of the model with respect to the measured values, for surge velocity and position.

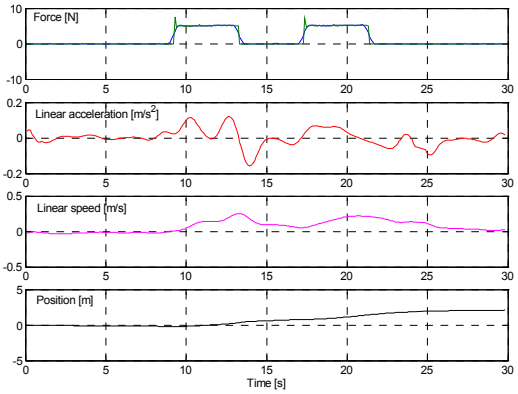

Fig. 3. Input signals for surge DOF (experiment 2)

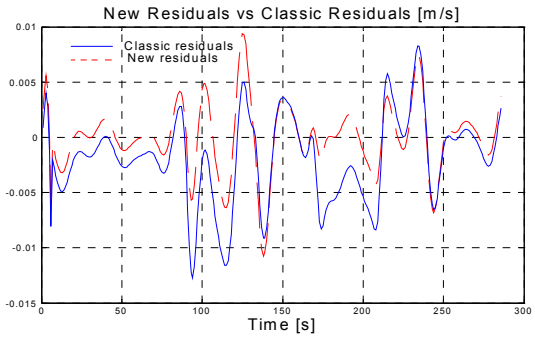

Fig. 4. Comparison of the residuals

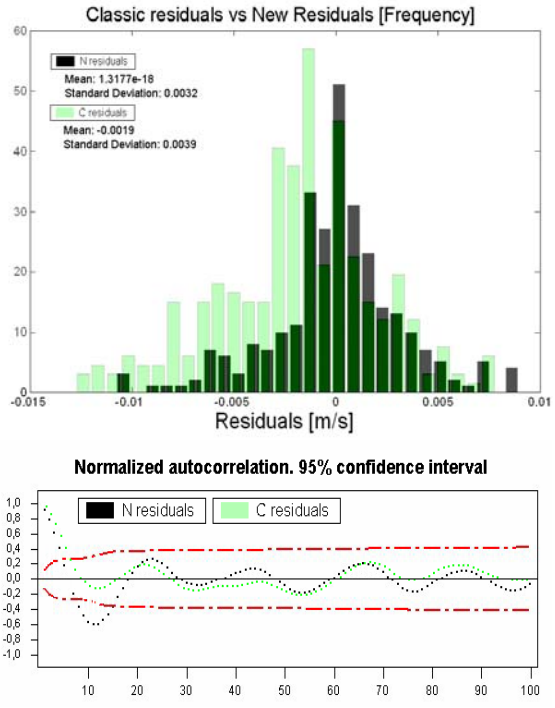

Fig. 5. Statistical validation for surge DOF (New vs. Classic)

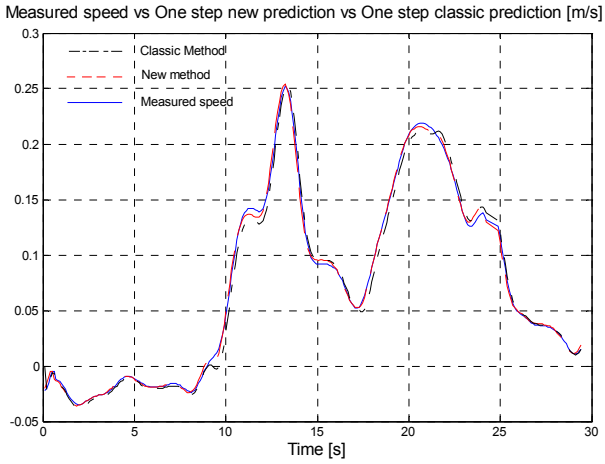

Fig. 6. One step speed simulation for surge DOF

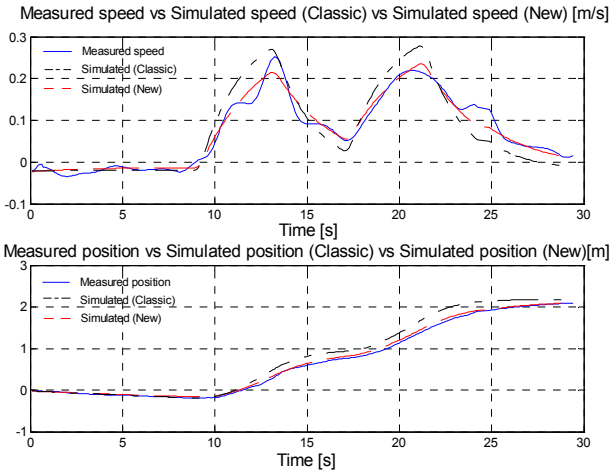

Fig. 7. Velocity and position response for surge DOF

4.2 Results for the rest of the identified DOF

Next tables and figures show the results obtained for the other two identified DOF. First we present the results for yaw DOF, where experiment 1 has been chosen to compare graphically both methods. Next, the results for pitch DOF are illustrated using experiment 1 for comparison.

Table 3 Parameter results for yaw DOF (New)

Exp		α_ψ	γ_ψ	δ_ψ	J_ψ
1	θ	1.1865	0.6261	-0.017	5.7759e-4
	σ	0.0031	0.0015	0.0006	
2	θ	1.3449	0.6178	0.1076	6.9684e-4
	σ	0.0053	0.0024	0.0010	
3	θ	1.1635	0.4221	-0.255	8.7854e-4
	σ	0.0029	0.0010	0.0011	
4	θ	1.2326	0.3468	0.1268	0.0020
	σ	0.0053	0.0014	0.0021	
Mean	θ	1.2426	0.5173	-0.050	8.38e-04
	σ	0.00355	0.00145	0.001	

Table 4 Parameter results for yaw DOF (Old)

Exp		α_ψ	γ_ψ	δ_ψ	J_ψ
1	θ	1.3755	0.7564	-0.0964	9.7534e-4
	σ	0.0052	0.0026	0.0010	
2	θ	1.1785	0.4549	-0.4069	0.0033
	σ	0.0082	0.0021	0.0035	
3	θ	1.1279	0.4936	0.2892	0.0032
	σ	0.0109	0.0036	0.0041	
4	θ	1.7541	0.5038	-0.9643	0.0082
	σ	0.0216	0.0058	0.0084	
Mean	θ	1.3590	0.5522	-0.2946	0.0039
	σ	0.0114	0.0035	0.0043	

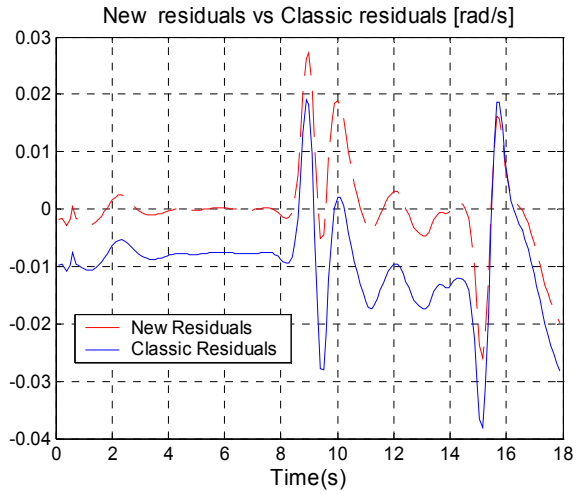

Fig. 8. Comparison of the residuals for yaw DOF

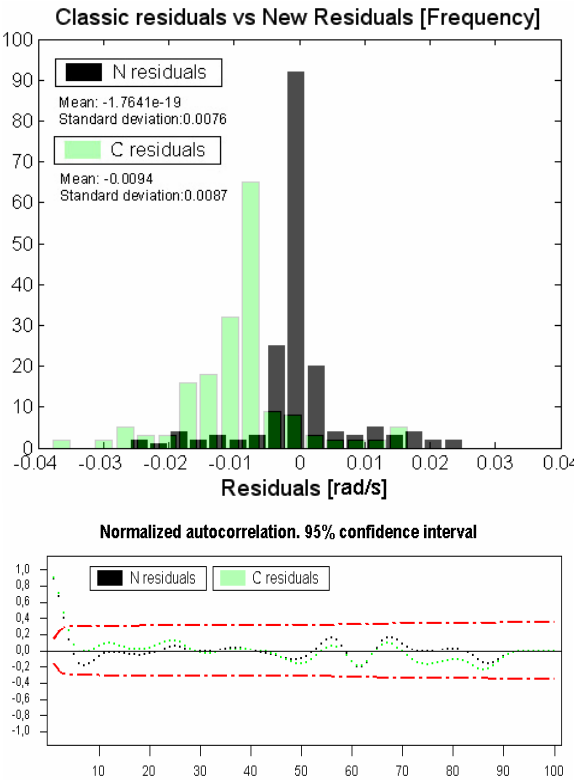

Fig. 9. Statistical validation for yaw DOF (New vs. Classic)

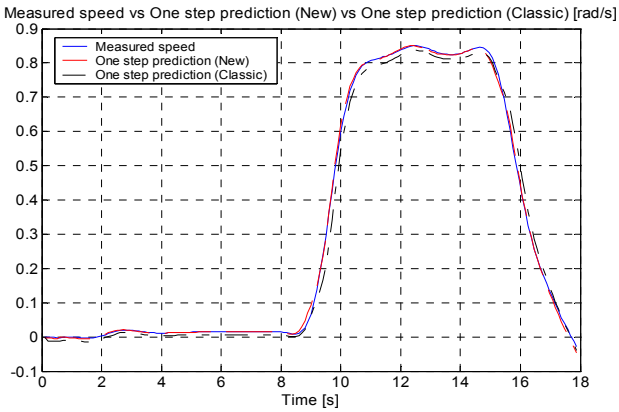

Fig. 10. One step speed simulation for yaw DOF

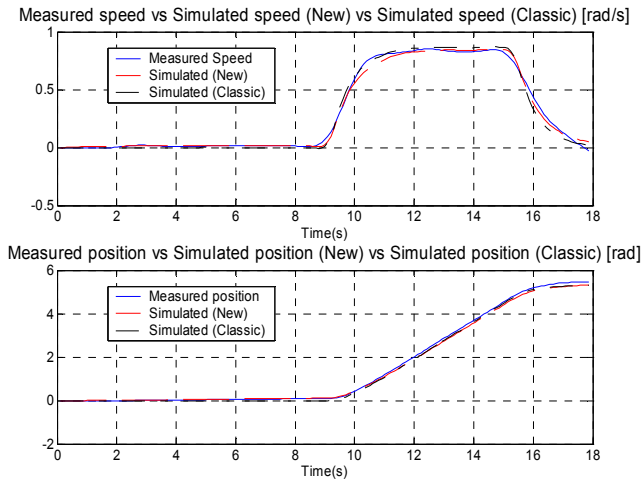

Fig. 11. Velocity and position response for yaw DOF

Table 5 Parameter results for pitch DOF (New)

Exp		α_θ	γ_θ	J_θ
1	θ	0.6486	1.0175	6.4228e-4
	σ	0.0013	0.0007	
2	θ	0.6586	0.8697	4.3642e-4
	σ	0.0009	0.0004	
3	θ	0.6895	1.0735	5.3489e-4
	σ	0.0019	0.0011	
Mean	θ	0.66395	0.9885	5.5032e-4
	σ	0.0011	0.0006	

Table 6 Parameter results for pitch DOF (Old)

Exp		α_θ	γ_θ	J_θ
1	θ	0.5783	1.2121	9.3260e-4
	σ	0.0027	0.0017	
2	θ	0.6122	1.0417	6.7892e-4
	σ	0.0039	0.0024	
3	θ	0.7092	1.4555	9.0143e-4
	σ	0.0037	0.0026	
Mean	θ	0.6332	1.2364	8.3765e-4
	σ	0.0034	0.0022	

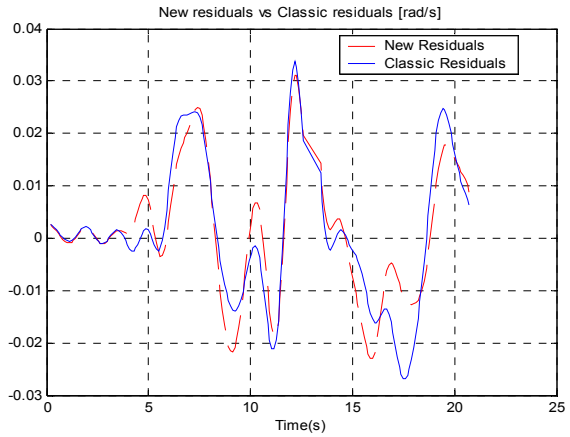

Fig. 12. Comparison of the residuals for pitch DOF

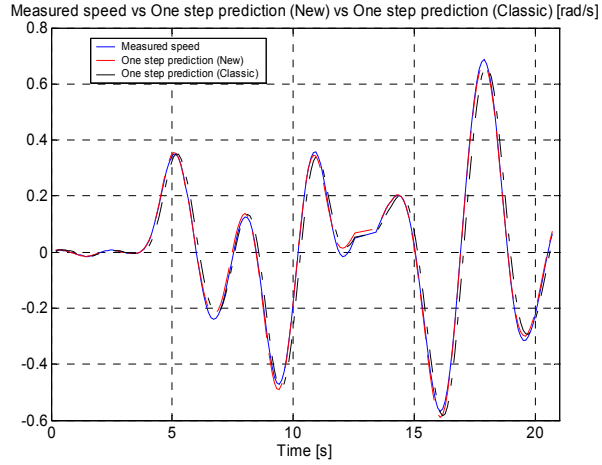

Fig. 13. One step speed simulation for pitch DOF

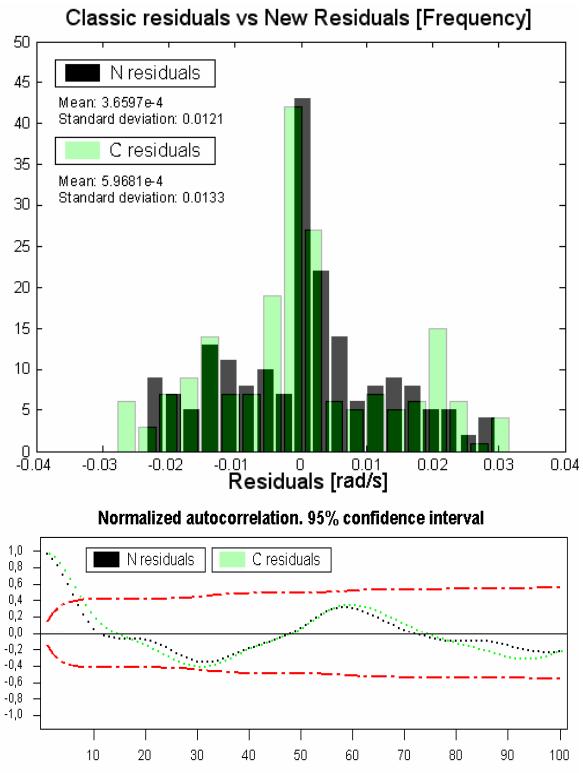

Fig. 14. Statistical validation for pitch DOF (New vs. Classic)

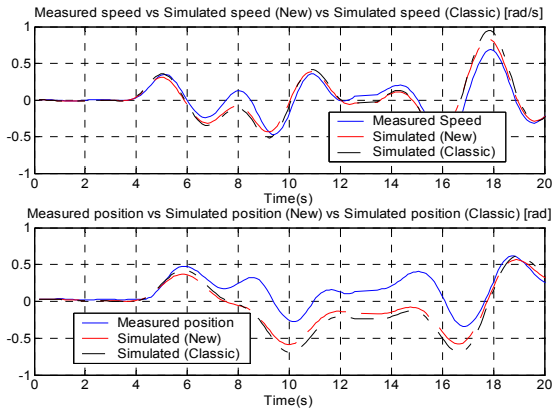

Fig. 15. Velocity and position response for pitch DOF

5 CONCLUSIONS

A comparison between two identification methods for a wide class of non linear systems has been presented. The both methods, operating off-line, have been applied to the identification of URIS UUV on the basis of real data. After an extensive set of experimental results, the new method has proven to perform better than the classic one. The new identified model has proven to be statistically good and will be used in the near future for simulation and control.

REFERENCES

A. Tiano, M. Carreras, P. Ridao and A. Zirilli, (2002). On the identification of non linear models of unmanned underwater vehicles. In: *10th Mediterranean Conference on Control and Automation*, Lisbon, Portugal.

Abkowitz, M.A., (1980). System identification techniques for ship manoeuvring trials. In: *Proceedings of Symposium on Control Theory and Navy Applications*, pp.337-393, Monterey, USA.

P. Ridao, J. Batlle and M. Carreras, (2001). Model identification of a low-speed UUV with on-board sensors. In: *IFAC conference CAMS'2001, Control Applications in Marine Systems*. Glasgow, Scotland, U.K.

Caccia, M., G. Indiveri and G. Veruggio (2000), Modelling and identification of open-frame variable configuration underwater vehicles, IEEE *Journal of Ocean Engineering*, **25**(2), pp.227-240.

Fossen, T.I., (1994). *Guidance and Control of Ocean Vehicles*, John Wiley and Sons, New York, USA.

Ljung, L., (1987). *System Identification :Theory for the User*, Prentice Hall, Englewoods Clifts.

M.Carreras, A.Tiano, A. El-Fakdi, A. Zirilli, P.Ridao, (2003). On the identification of non linear models of unmanned underwater vehicles. In: *1st IFAC Workshop on Guidance and Control of Underwater Vehicles GCUV '03*, Wales, UK.

Smallwood, D.A. and L.L. Whitcomb (2001). Preliminary experiments in the adaptive identification of dynamically positioned underwater robotic vehicles. In: *Proceedings of the IEEE/RSJ* International Conference on Intelligent Robots and Systems, pp.1803-1810 Maui, USA.